

# Fast calculation of a computer-generated hologram for RGB and depth images using a wavefront recording plane method

Naohisa Okada,<sup>1</sup> Tomoyoshi Shimobaba,<sup>1</sup> Yasuyuki Ichihashi,<sup>2</sup> Ryutaro Oi,<sup>2</sup> Kenji Yamamoto,<sup>2</sup> Takashi Kakue,<sup>1</sup> and Tomoyoshi Ito<sup>1</sup>

<sup>1</sup> Graduate School of Engineering, Chiba University, 1-33 Yayoi-cho, Inage-ku, Chiba 263-8522, Japan

<sup>2</sup> Universal Communication Research Institute, National Institute of Information and Communications Technology, 4-2-1 Nukui-Kitamachi, Koganei, Tokyo 184-8795, Japan

Received July 30, 2014; accepted September 04, 2014; published September 30, 2014

**Abstract**—In a three-dimensional display by a computer-generated hologram (CGH), fast computation of CGH is required. In this paper, in order to accelerate CGH generation, the following two methods are used; the first method is band-limited double-step Fresnel diffraction. Compared with convolution-based diffraction, such as an angular spectral method, the proposed method requires less computational time and memory. The second method is a wavefront recording plane (WRP) method which reduces the calculation amount by placing WRPs in the vicinity of an object. We succeeded in speeding up CGH calculation by combining both methods.

Electroholography is capable of reproducing three-dimensional (3D) moving images by displaying CGHs on an electronic display device [1], and is expected to be applied to realize an ultimate 3D television that can reproduce the wavefront of a 3D object. In addition to the problems of the image size and viewing zone, there is a problem that CGH calculation takes a long time. To solve this problem, many algorithms have been devised. For example, a method handling a 3D object as point light sources [2], method that treats a 3D object as polygons [3], method that deals with a multi-view image [4], and method that handles a 3D object as RGB-Depth (RGB-D) images [5].

We propose a fast CGH calculation method for RGB-D images in this research. We used RGB and depth images as shown in Fig. 1.



Fig. 1. RGB and depth images (a) RGB image (b) Depth image.

The RGB-D method first picks up the pixels in the RGB image with the same depth value in the depth image. As shown in Fig. 2, by picking up the pixels, we can generate parallel planes to the CGH with the same depth value. Then, this method performs 256 diffraction calculations from the parallel planes to the CGH iteratively due to the depth image having a value of 256.

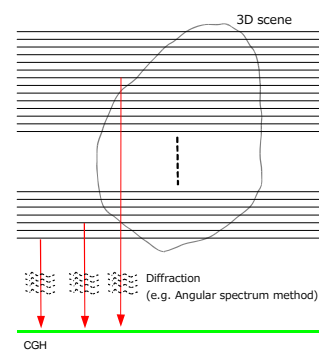


Fig. 2. RGB-D method.

Convolution-based diffraction such as the angular spectrum method takes much computational time and requires a lot of memory because convolution-based diffraction requires zero-padding to avoid circular convolution. Instead of convolution-based diffraction, using the band-limited double-step Fresnel diffraction (BL-DSF) can reduce memory usage and computational time [5]. BL-DSF originates from DSF [6]. DSF performs single-step Fresnel diffraction (SSF) which is calculated by the following equation,

$$u_2(m_2, n_2) = SSF_z[u_1(m_1, n_1)] = C_z FFT \left[ u_1(m_1, n_1) \exp \left( i \frac{\pi}{\lambda z} (x_1^2 + y_1^2) \right) \right] \quad (1)$$

where  $u_2(m_2, n_2)$  and  $u_1(m_1, n_1)$  are the source and destination plane,  $\lambda$  and  $z$  are the wavelength and propagation distance, and  $C_z$  is the complex coefficient.

SSF can be calculated by the Fast Fourier transform (FFT) once. Zero-padding is unrequired unlike with convolution-based diffraction; therefore, SSF is an efficient method in terms of computational time and memory required. However, the problem is that the sampling interval on the destination plane is changed by the propagation distance and the wavelength. To solve this problem, DSF has been devised. The calculation is performed by performing SSFs twice via a virtual plane, as shown in Fig. 3. DSF is expressed as

$$\begin{aligned}
 u_2(m_2, n_2) &= \text{DSF}[u_1(m_1, n_1)] \\
 &= \text{SSF}_{z_2} \left[ \text{SSF}_{z_1} [u_1(m_1, n_1)] \right].
 \end{aligned}
 \quad (2)$$

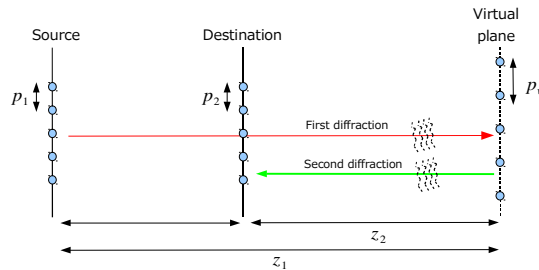


Fig. 3. Double step Fresnel diffraction.

DSF first performs light propagation with the distance of  $z_1$  from the source plane to the virtual plane by SSF. Next, DSF performs light propagation by SSF from the virtual plane to the destination plane at the propagation distance of  $z_2$ . The total propagation distance is  $z = z_1 + z_2$ . The sampling intervals of the source and destination planes are the same; unfortunately, DSF has the aliasing problem of the chirp functions included in DSF. In order to address this problem, we proposed BL-DSF, which enables calculation of the diffraction calculation without aliasing noise by introducing the band-limited function.

In order to obtain more speed, we use the combination of BL-DSF and our wavefront recording plane (WRP) method [7-9], which treats a 3D object as an aggregation of object points. This calculation model is shown in Fig. 4.

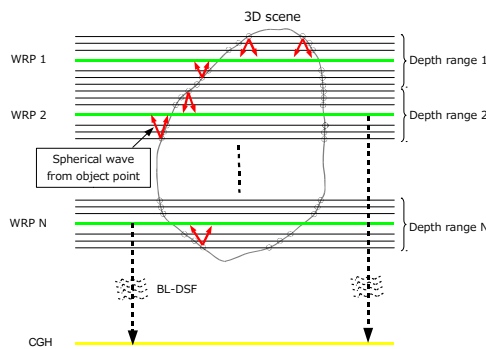


Fig. 4. Wavefront recording plane method.

The WRP method places a WRP near a 3D object. The complex amplitude on the WRP is calculated by superimposing spherical waves emitted from object points. If the WRP is located near a 3D object, this method can dramatically reduce the computational amount of the CGH because the spread of spherical waves is limited to small areas.

Since the amplitude and phase information of object points are recorded in the WRP, the diffraction calculation from the WRP to the CGH is equal to the case of calculating a complex amplitude on the CGH directly from

the object points. In Fig. 1, the RGB pixels in a parallel plane with the same depth value will be sparse rather than dense. In this case, regarding the RGB pixels as object points, the WRP method is faster than the diffraction calculation of the parallel plane.

In this proposed method, first, we generate multiple WRPs as shown in Fig. 4, and a WRP records a complex amplitude of object points within a certain depth range by superimposing spherical waves. The CGH calculation using multiple WRPs has been studied in the references [10,11]. However, these studies used convolution-based diffraction for the propagation of WRPs to the CGH. Instead, the proposed method uses BL-DSF for the propagation from the WRPs to the CGH. To the best of our knowledge, this is the first attempt to apply the WRP method to RGB-D images.

We show the calculation times and reconstructed image of a color CGH with  $8K \times 4K$  pixels generated by the angular spectrum method alone, BL-DSF alone and the proposed method. In the angular spectrum method we need to expand the size to  $16K \times 8K$ . The wavelengths of red, green and blue are 640nm, 532nm and 473nm, respectively. The propagation distance  $z$  is 0.03 m. The sampling interval is  $4.8\mu\text{m}$ .

Table 1 shows the computational times. In the proposed method, the number of WRPs we used is 32. We used a NVIDIA GeForce GTX 670 and Intel i5-3570 CPU (we used the CPU 4 threads). Note that N/A in the angular spectrum method alone in the GPU means that we cannot measure the calculation time because the calculation required is beyond the memory amount of the GPU.

Table 1. Computational times in the angular spectrum method alone, BL-DSF alone, and the proposed method.

	CPU(s)	GPU(s)
Angular spectrum method alone	10611	N/A
BL-DSF alone	2422	48.51
Proposed method (the combination of BL-DSF and WRP method)	487.6	15.67

We examined the number of WRPs. Table 2 shows the calculation time and the peak signal-to-noise ratio (PSNR) between the numerical reconstructed images by the proposed method and the angular spectrum method when changing the number of WRPs. The reconstructed image by the proposed method is shown in Fig. 5.



Fig. 5. The reproduced image by simulation.

Table 2. PSNR calculation time in each recording surface number.

Number of WRPs	CGH calculation time	PSNR
16	15.617 (s)	20.43
32	15.671(s)	20.45
64	20.688(s)	20.50
128	32.957(s)	20.43

As shown in Table 2, we adopted 32 WRPs because it showed good performance in both image quality and calculation time.

In addition, we created a CGH by decimating the pixels of the object points in the WRPs to further increase the computational speed. This was proposed in Ref. [12]. The influence of the decimation on the reconstructed image is small because the resolution of the reconstructed image of the CGH is beyond that of the human eye. Table 3 shows the calculation times and the PSNRs when changing decimation rates. For example, the decimation rate of 1/2 means that the number of object points is half of that original.

Table 3. PSNRs and computational times when changing the decimation rate.

Decimation rate	CGH calculation time (s)	PSNR
1	15.671	20.45
1/2	12.195	19.86
1/4	11.466	19.63
1/8	11.175	18.82
1/16	11.073	17.04

The degradation of the image quality is small when the decimation rate is 1/8. Figure 6 shows the reconstructed image with a decimation rate of 1/8. Compared to Fig. 5, the deterioration in image quality is small but the calculation time is 1.4 times faster.



Fig. 6. Reproduced image when decimating 1/8.

In this paper, we proposed fast CGH calculation using the combination of the WRP and BL-DSF. When the number of WRPs was 32, we obtained a higher calculation speed of 22 times in the CPU and 677 times in the GPU, compared with that of the angular spectrum method alone. In addition, when the decimation rate is 1/8, we obtained a

higher calculation speed of 950 times in the GPU, compared with that of the angular spectrum method alone.

This work is partially supported by JSPS KAKENHI Grant Numbers 25330125 and 25240015, and the Kayamori Foundation of Information Science Advancement and Yazaki Memorial Foundation for Science and Technology.

## References

- [1] T.C. Poon (Ed.), *Digital holography and three-dimensional display: Principles and Applications* (Springer, 2006).
- [2] S.C. Kim, E.S. Kim, *Appl. Opt.* **47**, D55 (2008).
- [3] K. Matsushima, H. Shimmel, F. Wyrowski, *J. Opt. Soc. Am. A.* **20**, 1755 (2003).
- [4] M. Yamaguchi, H. Hoshino, T. Honda, N. Ohya, *Proc. SPIE* **1914**, 25 (1993).
- [5] N. Okada, T. Shimobaba, Y. Ichihashi, R. Oi, K. Yamamoto, M. Oikawa, T. Kakue, N. Masuda, T. Ito, *Opt. Expr.* **21**, 9192 (2013).
- [6] F. Zhang, I. Yamaguchi, L.P. Yaroslavsky, *Opt. Lett.* **29**, 1668 (2004).
- [7] T. Shimobaba, N. Masuda, T. Ito, *Opt. Lett.* **34**, 3133 (2009).
- [8] T. Shimobaba, H. Nakayama, N. Masuda, T. Ito, *Opt. Expr.* **18** 19504 (2010).
- [9] J. Weng, T. Shimobaba, N. Okada, H. Nakayama, M. Oikawa, N. Masuda, T. Ito, *Opt. Expr.* **20**, 4018 (2012).
- [10] T. Shimobaba, T. Kakue, N. Masuda, Y. Ichihashi, K. Yamamoto and T. Ito, *Computer holography using wavefront recording method*, Digital Holography and Three-Dimensional Imaging (DH) DH2013, DTu1A. 2 (2013).
- [11] A.-H. Phan, M. -I. Piao, S. -K. Gil, N. Kim, *Appl. Opt.* **53**, 4817 (2014).
- [12] P. Tsang, W. -K. Cheung, T. -C. Poon, C. Zhou, *Opt. Expr.* **19**, 15205 (2011).